Vol 17 No 11, November 2008
1674-1056/2008/17(11)/4211-07

Chinese Physics B

© 2008 Chin. Phys. Soc.
and IOP Publishing Ltd

Dynamics of cooperative emissions in a cascade three-level molecular system driven by an ultrashort laser pulse*

Liu Ji-Cai(刘纪彩)[a)b)], Wang Chun-Xin(王春兴)[a)],
Gel'mukhanov Faris[b)], and Wang Chuan-Kui(王传奎)[a)b)†]

[a)] *College of Physics and Electronics, Shandong Normal University, Jinan* 250014, *China*

[b)] *Department of Theoretical Chemistry, School of Biotechnology, Royal Institute of Technology, SE*-10691 *Stockholm, Sweden*

(Received 6 February 2008; revised manuscript received 9 April 2008)

This paper investigates the dynamics of cooperative emissions in a cascade three-level system driven by an ultrashort laser pulse by solving numerically the full-wave Maxwell–Bloch equations. The 4, 4′-bis(dimethylamino) stilbene molecule is used as the model molecule because of its strong two-photon absorption property. The two-colour cooperative emissions are studied as functions of molecular number density and dephasing rate of the dipole coherence. The propagation effects on the evolution of the cooperative radiations are also taken into account. The cooperative radiations are enhanced for large number density of the molecule, while the fast dephasing of the dipole coherence reduces the intensity of the cooperative radiations and delays the emission times or even inhibits the formation of the emissions. The delay time of the radiation decreases with the increase of the molecular number density and the propagation distance.

Keywords: superfluorescence, ultra-short laser pulse, 4, 4′-bis(dimethylamino) stilbene organic molecule, Maxwell–Bloch equations

PACC: 4265, 3120A

1. Introduction

Since the pioneering work of Dicke[1] which predicted the cooperative emission of coherent radiation in an ensemble of completely inverted two-level systems, the collective emission phenomenon has attracted intense theoretical and experimental interest,[2−9] because the correlated investigations can give us a profound understanding of interaction between matter and light field. The cooperative effects involve many inverted atoms and change the nature of the spontaneous emission. The inverted medium can radiate its energy through typically two different ways: one is superfluorescence (SF), and the other is called amplified spontaneous emission (ASE). SF is non-stationary emission, where the formation and growth of the macroscopic dipole moment is expected. In contrast, ASE is quasi-stationary emission, where the formation of the macroscopic dipole moment is prevented due to the fast dephasing of the coherence between individual dipole. However, if the number density of the inverted atoms is large enough, the spontaneous emission from a single atom is amplified as the radiation propagates through the inverted medium.

There are basically two types of theoretical methods to investigate the cooperative emission. In the semi-classical theory, the emission of the coherent radiation is described by the Maxwell–Schrödinger or Maxwell–Bloch equations, and the initiation of the emission is induced by a fluctuating polarization source.[10−13] In the fully quantum-mechanical theory, the Heisenberg equations of motion for the field and microscopic atomic operators are used, and the radiation is initiated by zero-point fluctuations of the vacuum field.[14,15] Most of the previous studies used the slowly varying amplitude approximation (SVEA) and the rotating-wave approximation (RWA), as well as the linear approximation where the depletion of the upper level population is assumed to be much smaller than one. However, in the region of ultrastrong and ultrashort laser physics, the SVEA and RWA have al-

*Project supported by National Basic Research Program for China (Grant No 2006CB806000), Swedish Research Council, Carl Tryggers Stiftelse Foundation, Swedish International Development Cooperation Agency (SIDA),and Natural Science Foundation of Shandong Province of China (Grant No Z2007A02).

†Corresponding author. E-mail: ckwang@sdnu.edu.cn

ready broken down.[16−21] Moreover, the linear theory is also not valid anymore since the decrease of the upper level population can be considerably large.

In this paper, we investigate theoretically the dynamics of cooperative emissions in a cascade three-level system excited by an ultrashort laser pulse using the full-wave Maxwell–Bloch equations in which the classical fields are treated strictly with the Maxwell equations and the quantized optical active medium is described by the Bloch equations beyond the SVEA and RWA. The 4, 4′-bis(dimethylamino) stilbene is chosen here as the model molecule because of its strong two-photon absorption (TPA) property.[20,22] Electronic structure calculations show that in infrared and optical regions the molecule can be considered as a cascade three-level system, marked by S_0, S_1 and S_2 with energy levels $E_0 < E_1 < E_2$. Using an iterative predictor–corrector finite-difference time-domain method (FDTD),[17,18] we solve numerically the mutually coupled full-wave Maxwell–Bloch equations. The population inversion of the molecular medium is driven by an ultrashort laser pulse which is in two-photon resonance with the TPA transition between the ground (S_0) and the highest (S_2) levels. The dynamics of two-colour SF are studied for different number densities and dephasing rates of the molecular medium. Effects of pulse propagation on the emission of the cooperative radiations are also discussed in detail.

2. Theoretical tools: full-wave Maxwell–Bloch equations

Let us start from the density matrix equations in which the relaxation effects are taken into account phenomenologically,[23]

$$\frac{\partial \rho_{mn}}{\partial t} = -\frac{\mathrm{i}}{\hbar}[\hat{H},\rho]_{mn} - \gamma_{mn}\rho_{mn} \quad (m \neq n),$$

$$\frac{\partial \rho_{nn}}{\partial t} = -\frac{\mathrm{i}}{\hbar}[\hat{H},\rho]_{nn} + \sum_{E_m > E_n} \Gamma_{nm}\rho_{mm} - \sum_{E_m < E_n} \Gamma_{mn}\rho_{nn}. \tag{1}$$

Here γ_{mn} is the decay rate of the coherence ρ_{mn} related with the formation of the macroscopic dipole moment, and Γ_{mn} is the decay rate of the population from the energy level n to m. The decay of the coherence consists of two qualitatively different contributions,

$$\gamma_{mn} = \frac{\Gamma_m + \Gamma_n}{2} + \gamma_{mn}^{\mathrm{ph}}, \tag{2}$$

where $\Gamma_m = \sum_{E_{m'} < E_m} \Gamma_{m'm}$ and $\Gamma_n = \sum_{E_{n'} < E_n} \Gamma_{n'n}$ are respectively the total decay rates of populations out of levels m and n which usually do not depend on the number density of the medium, whereas the dipole dephasing rate $\gamma_{mn}^{\mathrm{ph}}$ is proportional to the number density of the medium[24]

$$\gamma_{mn}^{\mathrm{ph}} \simeq \bar{v}\sigma_{mn}N, \tag{3}$$

where σ_{mn} is the cross section of the dephasing collisions of the absorbing molecule with the solvent particles and $\bar{v}$ is the thermal velocity, and N is the number density of the molecule. Within the electric dipole approximation, the total Hamiltonian $\hat{H}$ is the sum of the free system Hamiltonian $\hat{H}_0$ and the interaction Hamiltonian $\hat{V}(t,z) = -\boldsymbol{\mu}\cdot\boldsymbol{E}$ of the medium with the external field $\boldsymbol{E}$, where $\boldsymbol{\mu}$ is the electric dipole moment operator of the medium.

For a three-level system, using the following substitution in Eq.(1):

$$\begin{aligned} \rho_{01} &= \frac{u_0 + \mathrm{i}v_0}{2}, \\ \rho_{12} &= \frac{u_1 + \mathrm{i}v_1}{2}, \\ \rho_{02} &= \frac{u_2 + \mathrm{i}v_2}{2}, \end{aligned} \tag{4}$$

we obtain the corresponding Bloch equations,

$$\begin{aligned} \frac{\partial u_0}{\partial t} &= -\omega_{10}v_0 + \frac{\boldsymbol{E}\cdot(\boldsymbol{\mu}_{11}-\boldsymbol{\mu}_{00})v_0}{\hbar} + \frac{\boldsymbol{E}\cdot(\boldsymbol{\mu}_{12}v_2+\boldsymbol{\mu}_{02}v_1)}{\hbar} - \gamma_{01}u_0, \\ \frac{\partial v_0}{\partial t} &= \omega_{10}u_0 - \frac{\boldsymbol{E}\cdot(\boldsymbol{\mu}_{11}-\boldsymbol{\mu}_{00})u_0}{\hbar} - \frac{\boldsymbol{E}\cdot(\boldsymbol{\mu}_{12}u_2-\boldsymbol{\mu}_{02}u_1)}{\hbar} - \frac{2}{\hbar}\boldsymbol{E}\cdot\boldsymbol{\mu}_{01}(\rho_{00}-\rho_{11}) - \gamma_{01}v_0, \\ \frac{\partial u_1}{\partial t} &= -\omega_{21}v_1 + \frac{\boldsymbol{E}\cdot(\boldsymbol{\mu}_{22}-\boldsymbol{\mu}_{11})v_1}{\hbar} - \frac{\boldsymbol{E}\cdot(\boldsymbol{\mu}_{02}v_0+\boldsymbol{\mu}_{01}v_2)}{\hbar} - \gamma_{12}u_1, \\ \frac{\partial v_1}{\partial t} &= \omega_{21}u_1 - \frac{\boldsymbol{E}\cdot(\boldsymbol{\mu}_{22}-\boldsymbol{\mu}_{11})u_1}{\hbar} - \frac{\boldsymbol{E}\cdot(\boldsymbol{\mu}_{02}u_0-\boldsymbol{\mu}_{01}u_2)}{\hbar} - \frac{2}{\hbar}\boldsymbol{E}\cdot\boldsymbol{\mu}_{12}(\rho_{11}-\rho_{22}) - \gamma_{12}v_1, \end{aligned}$$

$$\begin{aligned}
\frac{\partial u_2}{\partial t} &= -\omega_{20} v_2 + \frac{\boldsymbol{E}\cdot(\boldsymbol{\mu}_{22}-\boldsymbol{\mu}_{00})v_2}{\hbar} + \frac{\boldsymbol{E}\cdot(\boldsymbol{\mu}_{12}v_0-\boldsymbol{\mu}_{01}v_1)}{\hbar} - \gamma_{02}u_2,\\
\frac{\partial v_2}{\partial t} &= \omega_{20} u_2 - \frac{\boldsymbol{E}\cdot(\boldsymbol{\mu}_{22}-\boldsymbol{\mu}_{00})u_2}{\hbar} - \frac{\boldsymbol{E}\cdot(\boldsymbol{\mu}_{12}u_0-\boldsymbol{\mu}_{01}u_1)}{\hbar} - \frac{2}{\hbar}\boldsymbol{E}\cdot\boldsymbol{\mu}_{02}(\rho_{00}-\rho_{22}) - \gamma_{02}v_2,\\
\frac{\partial \rho_{00}}{\partial t} &= \frac{\boldsymbol{E}}{\hbar}\cdot(\boldsymbol{\mu}_{01}v_0+\boldsymbol{\mu}_{02}v_2) + \Gamma_{01}\rho_{11},\\
\frac{\partial \rho_{11}}{\partial t} &= -\frac{\boldsymbol{E}}{\hbar}\cdot(\boldsymbol{\mu}_{01}v_0-\boldsymbol{\mu}_{12}v_1) - \Gamma_{01}\rho_{11} + \Gamma_{12}\rho_{22},\\
\frac{\partial \rho_{22}}{\partial t} &= -\frac{\boldsymbol{E}}{\hbar}\cdot(\boldsymbol{\mu}_{02}v_2+\boldsymbol{\mu}_{12}v_1) - \Gamma_{12}\rho_{22},
\end{aligned} \tag{5}$$

where $\boldsymbol{\mu}_{mn} = \boldsymbol{\mu}_{nm}$ $(m,n = 0,1,2)$ are the matrix elements of the permanent electric dipole moments $(m = n)$ or of the transition electric dipole moments $(m \neq n)$, and $(\hat{H}_0)_{mn} = \hbar\omega_{mn}$ is the transition energy between the states m and n.

With the assumption that the polarization vector of the incident field is along x-axis and that the field propagates along z-axis, the one-dimensional Maxwell equations can be written as

$$\begin{aligned}
\frac{\partial E_x}{\partial z} &= -\mu_0\frac{\partial H_y}{\partial t},\\
\frac{\partial H_y}{\partial z} &= -\frac{\partial P_x}{\partial t} - \varepsilon_0\frac{\partial E_x}{\partial t},
\end{aligned} \tag{6}$$

where μ_0 and ε_0 are respectively the permeability and permittivity of free space, P_x is the x component of the macroscopic dipole moment $\boldsymbol{P}$. The macroscopic dipole moment is related to the ensemble average of the expectation value of the dipole moment operator,

$$\boldsymbol{P} = N < \boldsymbol{\mu} >= N\mathrm{tr}(\boldsymbol{\mu}\rho). \tag{7}$$

For a three-level system, with the substitutions of Eq.(4), $\boldsymbol{P}$ equals to

$$\begin{aligned}
\boldsymbol{P} =& N(\boldsymbol{\mu}_{01}u_0 + \boldsymbol{\mu}_{12}u_1 + \boldsymbol{\mu}_{20}u_2 + \boldsymbol{\mu}_{00}\rho_{00}\\
&+ \boldsymbol{\mu}_{11}\rho_{11} + \boldsymbol{\mu}_{22}\rho_{22}).
\end{aligned} \tag{8}$$

3. Computational details

The Maxwell equations (6) and the Bloch equations (5) couple with each other through the macroscopic dipole moment $\boldsymbol{P}$ expressed in Eq.(8). In simulations, we solve numerically the three-level Maxwell–Bloch equations with the FDTD and predictor-corrector methods.[17,18] The 4, 4′-bis(dimethylamino) stilbene is used as the nonlinear medium because the ab initio calculation[20] shows that this strong TPA molecule can be well described by a cascade three-level model in low energy region. The transition dipole moments between the ground state (S_0) and the first excited state (S_1) and between S_1 and the TPA state S_2 along x-axis are $\mu_{10}^x = 10.433$ Debye and $\mu_{21}^x = 18.497$ Debye, respectively, while the other components are approximately equal to zero due to the planarity of the molecule. The transition between S_2 and S_0 is dipole forbidden, $\boldsymbol{\mu}_{20} = 0$. The permanent dipole moments of these states are also equal to zero in the 4, 4′-bis(dimethylamino) stilbene which has a one-dimensional symmetrical characteristic. The excitation energies of the S_1 and S_2 states are $\hbar\omega_{10} = 3.46$ eV and $\hbar\omega_{20} = 4.27$ eV. The molecule is assumed to be rest in its ground state S_0 and there is no coherence between states before the excitation laser pulse is switched on, namely $\rho_{00} = 1$, $\rho_{11} = \rho_{22} = 0$ and $\rho_{mn} = 0$ $(m \neq n)$. The lowest excited electronic state always has a long lifetime ($\sim$ 1 ns), while it is much shorter for the higher excited states ($\leq$ 1 ps).[24] In simulations, $1/\Gamma_{01} = 1$ ns and $1/\Gamma_{12} = 1$ ps are used. And the decay rates of the dipole coherence are assumed to be the same for all transitions, $\gamma_{01} = \gamma_{12} = \gamma_{02} = \gamma$.

The incident excitation pulse is modelled with a hyperbolic-secant shape

$$\begin{aligned}
&E_x(t = 0, z)\\
=&F_0\mathrm{sech}[1.76(z/c + z_0/c)/\tau]\cos[\omega(z + z_0)/c],
\end{aligned}$$

where F_0 is the peak amplitude of the pulse, τ is the full width at half maximum (FWHM) of the intensity profile of the pulse. The carrier-wave frequency of the incident field is taken to be half of the frequency between the S_2 and S_0 states ($\omega = \omega_{20}/2$), i.e. the two-photon resonant frequency of the TPA process. It is worthwhile to point out that the field $\boldsymbol{E}$ in the Maxwell–Bloch equations (5) and (6) is the total field, including both the excitation field and the cooperative emitted radiations.[19] In the following numerical simulations, the FWHM of the incident excitation pulse

τ is set to be 5 fs, and the peak amplitude F_0 of the pulse are chosen as 4.0×10^7 V/cm. The corresponding two-photon area of the pulse is $\theta_0 = 1.4\pi$. Since the two-photon area theorem[19] was obtained within the two-photon RWA which breaks down for the intense ultrashort laser pulse, there are only about 90% populations of the ground state S_0 which are excited to the TPA state S_2 by the 1.4π driving pulse. The attenuation of the excitation pulse during its propagation is also taken into account, which means that the degree of the population inversion becomes weaker and weaker through pulse propagation. However, since the spatial and temporal evolution of the two-photon resonant pulse has been investigated in detail in Ref.[20], here we will mainly pay attention to the cooperative emission of radiations.

4. Results and discussion

The temporal evolution of the field after propagating 7.0 μm in the molecular medium with different number densities is shown in Fig.1. The decay rate γ of the dipole coherence is 1×10^{13} /s. The forefront pulse in each panel of Fig.1 is the excitation one, and the following parts are the emitted cooperative radiations of the medium inverted by the two-photon coherent excitation. One can see from Fig.1 that with the increase of the molecular number density, the intensity of the cooperative emissions are also enhanced, and the delay time between the cooperative emissions and the excitation pulse decreases. As is expected, through spectrum analysis we have confirmed that the observed cooperative emissions in Figs.1(b)–1(c) belong to cascade two-colour SF.[25,26] The front edge of the radiation is mainly the SF centred at the resonant transition frequency ω_{21} between levels S_2 and S_1, and then the cascade SF of levels S_1 and S_0 with frequency ω_{10}. The two-colour SF radiations are not completely separated in time, for example, they mix with each other in the middle of the two radiation pulses in Fig.1(b), and the delay time between the initiation of the two-colour SF reduces for higher molecular number density. When the number density N is $7\times10^{20}/\mathrm{cm}^3$ (Fig.1(d)), there is almost no delay time both between the excitation pulse and the two-colour SF and between the two-colour cascade emissions. In this case, the excitation pulse is seriously deformed and is a little delayed with respect to the lower density cases (Figs.1(a)–1(c)). Furthermore, the spectrum is shifted because the four-wave mixing effects come into play and new frequency components such as $2\omega_{21} + \omega$ are generated.[27–29]

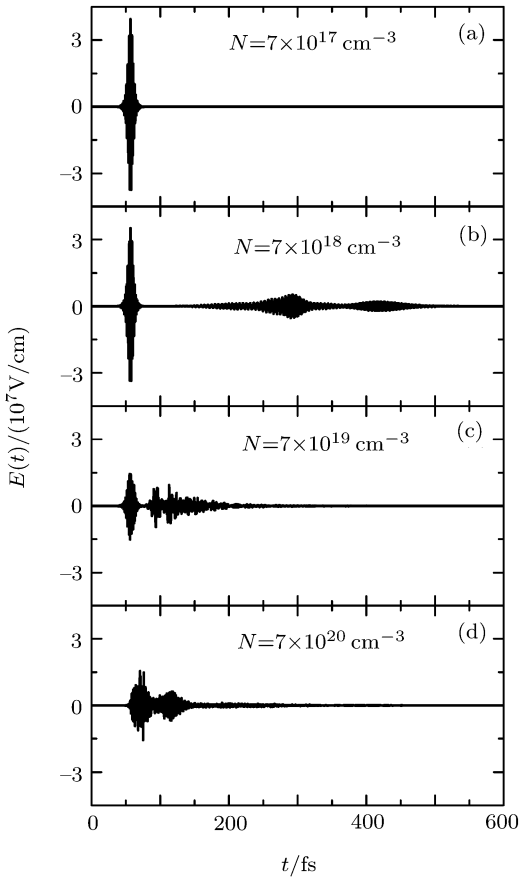


Fig.1. Temporal shape of the field after propagating 7.0 μm in the medium with different molecular number densities. The decay rate $\gamma = 1 \times 10^{13}$ /s. The FWHM of the excitation pulse $\tau = 5$ fs and the two-photon area of the pulse is $\theta_0 = 1.4\pi$.

The emission of the cooperative radiations as a function of the dephasing rate of the transition dipole moments is studied for different molecular number densities N, 7×10^{18} /cm^3 (Fig.2(a)) and 7×10^{19} /cm^3 (Fig.2(b)). One can see that with the increase of the dephasing rate, the intensity of the cooperative emission decreases, meanwhile the delay time increases. That is because the rapid dephasing rate of the coherence inhibits the formation of the macroscopic dipole moment and it takes a longer time for the individual molecule to become in-phase. Comparing Fig.2(a) and Fig.2(b), one can found that the intensity of the cooperative emissions is enhanced and the delay time is shortened for larger number density of the molecule. When the decay rate is 1×10^{12} /s, the dephasing of the dipole coherence is comparable with the lifetime broadening of the population (see Eq.(2)). In

this case, the macroscopic dipole moment has enough time to be formed before its growth is disturbed by the depletion of the population, so we can see in the upper-most panel of Fig.2(b) that an intense and short SF pulse with carrier-frequency ω_{10} is generated. The discontinuous long tail after the main SF radiation is interpreted as the ASE that is amplified along the propagation of the field.[5,10] When the decay rate increases to 1×10^{14} /s, it is difficult for the macroscopic dipole moment to be developed with a small molecular number density (Fig.2(a)), so there are only very weak spontaneous emissions due to the finite lifetime of the excited states. However, if we increase the molecular number density to 7×10^{19} /cm^3, a well-shaped pulse with frequency ω_{21} can be obtained in Fig.2(b). But there is still no cooperative emission at frequency ω_{10}, namely no macroscopic dipole moment between the first-excited state and the ground state is formed due to the fast decay of the coherence.

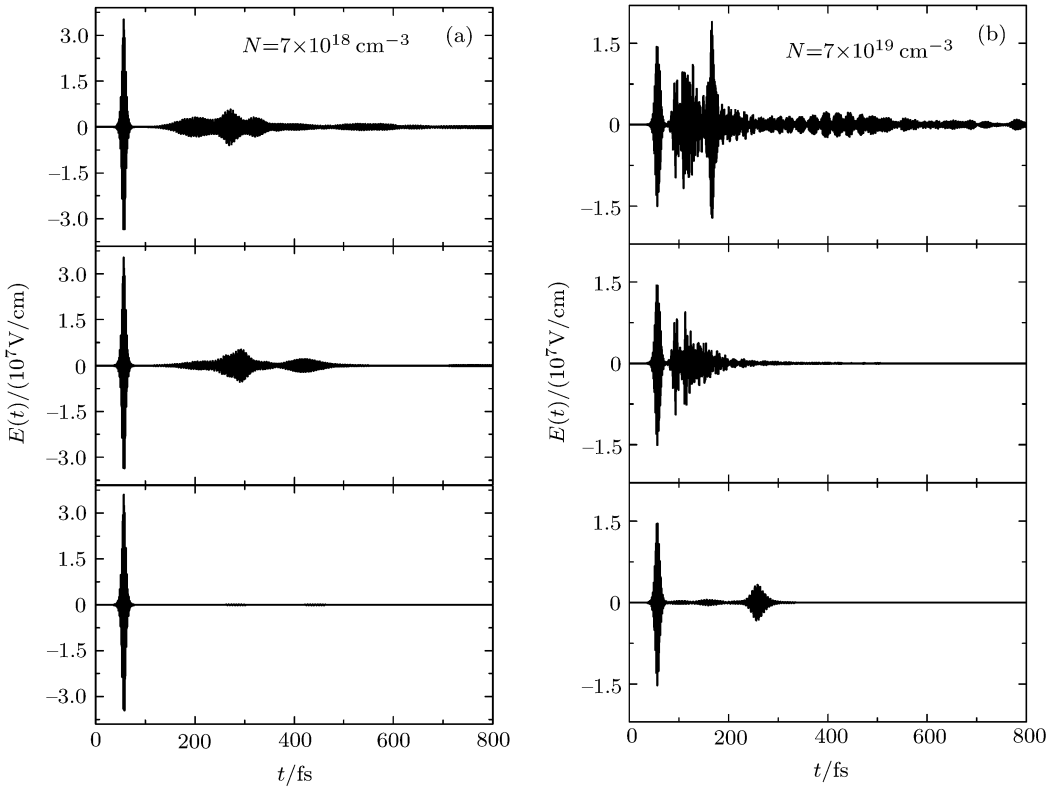


Fig.2. Influence of the dephasing rate of the coherence on the evolution of the field in the molecular media with the number densities to be 7×10^{18} / cm^3 (a) and 7×10^{19} /cm^3 (b). The decay rates γ are 1×10^{12} /s (upper panel), 1×10^{13} /s (middle panel) and 1×10^{14} /s (bottom panel), and the lifetime broadening of states S_1 and S_2 are 1 ns and 1 ps, respectively. $z=7.0\,\mu$m, $\tau=5$ fs, $\theta_0=1.4\pi$.

In order to give an insight into the physical mechanism of the cooperative emission, Fig.3 shows the temporal evolution of the populations $\rho(t)$ and of the macroscopic dipole moment $P(t)$ at different propagation distances. In the cascade three-level system, the population inversion between states S_2 and S_0 is achieved by an incident two-photon resonant pulse with a 1.4π pulse area, and the intermediate state S_1 is not populated initially by the excitation field. Figure 3(a) shows that at the beginning of the propagation, the depletion of the upper state populations $\rho_{22}(t)$ to the intermediate state S_1 is only caused by weak spontaneous emission, and there is no population transfer between the intermediate and the ground states due to the long lifetime of the first-excited state ($1/\Gamma_{01}$=1 ns). Correspondingly, the macroscopic dipole moment is negligible except for the forefront peak which is coherently induced by the incident laser pulse (Fig.3(b), z=0.014 μm). With the increase of the propagation distance, an emission process occurs that is qualitatively different from the spontaneous emission. The populations of the state S_2 are transferred suddenly into the intermediate state S_1 at the instance t_1, which indicates the burst of the SF between these

two levels. One can also see from Fig.3(b) that the macroscopic dipole moment is built up at t_1, which then becomes the source of the SF. The large population transfer from the upper state to the intermediate state initiates the population inversion between the intermediate and the ground sates. At a later time t_2, the SF emission between states S_1 and S_0 bursts, it is accompanied by the large population transfer from S_1 to S_0. The two characteristic times t_1 and t_2 are the delay times of the initiation of the two-colour SF with respect to the driving laser pulse and they decrease with further propagation of the field in the inverted medium.

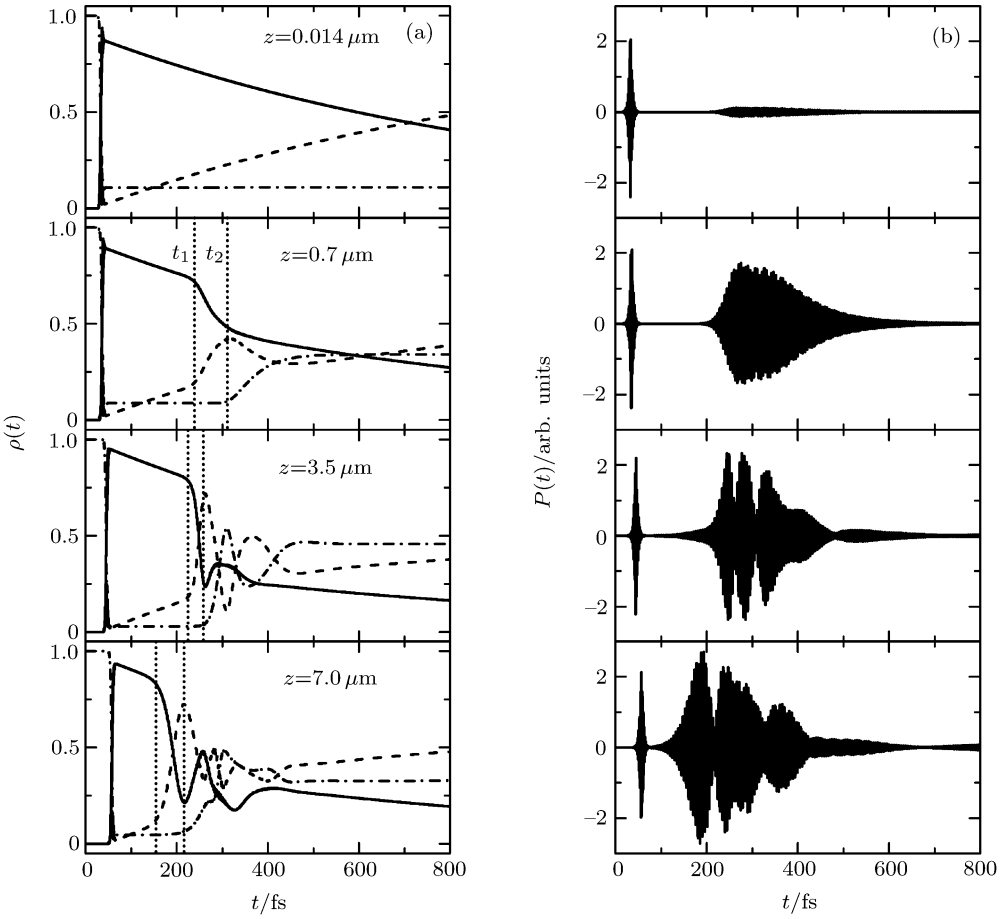


Fig.3. Temporal evolution of the population $\rho_{00}(t)$ (dash-dotted), $\rho_{11}(t)$ (dashed), $\rho_{22}(t)$ (solid) (a), and the formation of the macroscopic polarization $P(t)$ (b) with different propagation length z. $\gamma = 1 \times 10^{13}$ /s, $N = 7 \times 10^{18}$ /cm^3, $\tau = 5$ fs, $\theta_0 = 1.4\pi$.

Finally, we would like to point out that the emission of the cooperative radiations also depends strongly on the intensity of the incident driving pulse, since it determines the population inversion of the medium. We found that when the population inversion between the upper and the ground states excited by the two-photon driving pulse is very weak or even when no population inversion is achieved, yoked SF[6] other than the cascade two-colour SF is formed for slowly dephasing rates. In the case of yoked SF, the emission of the SF from the upper and lower transitions bursts simultaneously due to the coupling of the upper emissions with the coherent superposition state of the two-photon excited molecules. On the other hand, with high enough dephasing of the dipole coherence only SF between the upper and the intermediate states with ω_{21} frequency is emitted in this case due to the lack of population inversion between the intermediate and the ground states.

5. Conclusions

We have studied theoretically the dynamics of cooperative emissions in a cascade three-level system driven by an ultrashort laser pulse by use of the semi-

classical theory. The full-wave Maxwell–Bloch equations beyond the SVEA and RWA are solved numerically with the iterative predictor–corrector FDTD method. The strong TPA organic molecule 4, 4′-bis(dimethylamino) stilbene is selected as the model system. The incident laser pulse tuned in two-photon resonance with medium provides the initial population inversion between the upper and the ground states of the cascade three-level system. It is found that the intensity of the two-colour cascade cooperative radiations are enhanced for large molecular number density, on the other hand the fast dephasing of the dipole coherence reduces the intensity of the cooperative radiations and delays the emission times or even inhibits the formation of the emissions. The delay time of the radiation decreases with the increase of the number density and the length of the nonlinear molecular medium due to the faster formation of the macroscopic dipole moment.

References

[1] Dicke R H 1954 *Phys. Rev.* **93** 99

[2] Gross M and Haroche S 1982 *Phys. Rep.* **93** 301

[3] Gibbs H M, Vrehen Q H F and Hikspoors H M J 1977 *Phys. Rev. Lett.* **39** 547

[4] Haake F, Haus J, King H and Schröder G 1980 *Phys. Rev. Lett.* **45** 558

[5] Malcuit M S, Maki J J, Simkin D J and Boyd R W 1987 *Phys. Rev. Lett.* **59** 1189

[6] Brownell J H, Lu X and Hartmann S R 1995 *Phys. Rev. Lett.* **75** 3265

[7] Frolov S V, Gellermann W, Ozaki M, Yoshino K and Vardeny Z V 1997 *Phys. Rev. Lett.* **78** 729

[8] Kimberg V, Polyutov S, Gel'mukhanov F, Ågren H, Baev A, Zheng Q D and He G S 2006 *Phys. Rev.* A **74** 033814

[9] He G S, Lu C G, Zheng Q D, Baev A, Samoc M and Prasad P N 2006 *Phys. Rev.* A **73** 033815

[10] Okada J, Ikeda K and Matsuoka M 1978 *Opt. Commun.* **26** 189
Okada J, Ikeda K and Matsuoka M 1978 *Opt. Commun.* **27** 321

[11] Trallero-Herrero C, Spanner M and Weinacht T 2006 *Phys. Rev.* A **74** 051403(R)

[12] Meziane J, Oullemine S, Amezian K and Boursey E 2002 *Chem. Phys. Lett.* **363** 573

[13] Kozlov V, Kocharovskaya O, Rostovtsev Y and Scully M 1999 *Phys. Rev.* A **60** 1598

[14] Haake F and Reibold R 1984 *Phys. Rev.* A **29** 3208

[15] Schuurmans M F H 1980 *Opt. Commun.* **34** 185

[16] Hughes S 1998 *Phys. Rev. Lett.* **81** 3363

[17] Ziolkowski R W, Arnold J M and Gobny D M 1995 *Phys. Rev.* A **52** 3082

[18] Tarasishin A V, Magnitskii V A, Shuvaev V A and Zheltikov A M 2001 *Opt. Express* **8** 452

[19] Liu J C, Wang C K and Gel'mukhanov F 2007 *Phys. Rev.* A **76** 043422
Liu J C, Wang C K and Gel'mukhanov F 2007 *Phys. Rev.* A **76** 053804

[20] Wang C K, Liu J C, Zhao K, Sun Y P and Luo Y 2007 *J. Opt. Soc. Am.* B **24** 2436

[21] Liu J C, Zhao K, Song Y Z and Wang C K 2006 *Acta Phys. Sin.* **55** 1803 (in Chinese)

[22] Albota M, Beljonne D, Brédas J L, Ehrlich J E, Fu J Y, Heikal A A, Hess S E, Kogej T, Levin M D, Marder S R, McCord-Maughton D, Perry J W, Röckel H, Rumi M, Subramaniam G, Webb W W, Wu X L and Xu C 1998 *Science* **281** 1653

[23] Boyd R W 2003 *Nonlinear Optics* (San Diego: Elsevier)

[24] Gel'mukhanov F, Baev A, Macák P, Luo Y and Ågren H 2002 *J. Opt. Soc. Am.* B **19** 937

[25] Ikeda K, Olada J and Marsuoka M 1980 *J. Phys. Soc. Jpn.* **48** 1636
Ikeda K, Olada J and Marsuoka M 1980 *J. Phys. Soc. Jpn.* **48** 1646

[26] Gross M, Fabre C, Pillet P and Haroche S 1976 *Phys. Rev. Lett.* **36** 1035

[27] Boyd R W, Michelle M S and Gauthier D J 1987 *Phys. Rev.* A **35** 1648

[28] Lvovsky A I, Hartmann S R and Moshary F 1999 *Phys. Rev. Lett.* **82** 4420

[29] Malcuit M S, Gauthier D J and Boyd R W 1985 *Phys. Rev. Lett.* **55** 1086